Comparisons of 3D Shape Clustering with Different Face Area Definitions

Jianwei Niu[1,*], Zhizhong Li[2], and Song Xu[2]

[1] School of Mechanical Engineering, University of Science and Technology Beijing, Beijing, 100083, China
Tel.: 86-131-61942805
niujw03@gmail.com, niujw@me.ustb.edu.cn
[2] Department of Industrial Engineering, Tsinghua University, Beijing, 100084, China
zzli@tsinghua.edu.cn, thusteven@gmail.com

Abstract. The importance of fit for face-related wearing products has introduced the necessity for better definition of face area. In this paper, three definitions of face area are compared on the context of Three dimensional (3D) face shape similarity based clustering. The first method defines the face area by spanning from the whole head grid surface by the front π/2 wedge angle along a line going through the centroid and pointing to the top of the head. The second method defines the face area as the grid surface enclosed by several anthropometric landmark points (sellion, both zygions, and menton) on the facial surface. The zonal surface where the respirator interferes with the wear's face is taken as the third alternative definition for the comparative study. By utilizing the block-distance measure, each face was converted into a compact block-distance vector. Then, k-means clustering was performed on the vectors. 376 3D face data sets were tested in this study. One-way ANOVA on the block distance based vectors was conducted to evaluate the influence on clustering results by utilizing different face area definitions. No difference was found at the significant level of 0.05. However, the cluster membership shows great difference between different definitions. This emphasizes the value of the selection of face area in 3D face shape-similarity-based clustering.

Keywords: 3D anthropometry; face area; shape comparison; clustering.

1 Introduction

Of all the biometrics features, face is among the most common ones [1]. Face anthropometry is a focused issue over the past years. It has applications in clinical diagnostics, cosmetic surgery, forensics, arts and other fields. For example, comparison with patient's face anthropometric data can help to indicate the existence of deformities, possibly leading to discovery of an illness [2]. If size and shape of a deformity are quantifiable, the surgeon can make more exact statements about necessary corrections [3]. Before 3D digitalizing technology emerged, traditional anthropometry was based on one-dimensional (1D) dimensions. Fortunately, with the wide availability of 3D

* Corresponding author.

V.G. Duffy (Ed.): Digital Human Modeling, HCII 2009, LNCS 5620, pp. 55–63, 2009.

scanning technologies, it is convenient to acquire the 3D data of the human body. Understanding the 3D shape variation is essential to many scientific activities such as personal identification, population accommodation, human computer interaction, and image retrieval, etc [4]. Extraction of biologically important information on shape variance from 3D digitized samples has been developed as geometric morphometrics, which has now found extensive applications to 3D human data, such as pathology, archaeology, primatology, paleoanthropology, and reconstructive craniofacial surgery [5]. For example, Hennessy et al. [6] made an effort by using 3D face shape to establish a relationship between facial morphogenesis and adult brain function as a basis for conducting subsequent studies in schizophrenia.

How to use 3D anthropometry to obtain proper fit of wearing products has been excessively addressed [7-11], while how to use 3D face anthropometry for the fit design purpose has not been well investigated yet. As an example, Mochimaru and Kouchi [12] used Free Form Deformation (FFD) method in the analysis of 3D human face forms for spectacle frames design.

As typical face-related wearing products, respirators have been widely used across numerous fields. The current sizing for respirators is based on some linear measurements. In USA, the respirator RFTP with the proper facial anthropometric dimensions should specify tightness of fit satisfactorily for >95% of the targeted race group [13, 14]. However, NIOSH's research indicated that the LANL panel for full-facepiece respirators accommodated only 84% of current civilian subjects [15]. Utilizing 3D facial shape information appears to be a promising avenue to overcome some of the limitations of current 1D-measurement based sizing systems and widened the opportunities for improving the design of face-related products. However, unlike some other biometrics features such as iris, retina, and fingerprint, it's usually difficult to define the face area strictly, especially in 3D form. Various definitions of face area have been introduced in the past. There is considerable interest in the assessment of 3D shape clustering with different face area definitions. In this paper, three definitions of face area are compared on the context of 3D face shape similarity based clustering.

The remainder of this paper is organized as follows. In Section 2, we introduce the method. Section 3 reports the results and gives some discussions. Finally, Section 4 summarizes this study.

2 Methods

2.1 Different Face Area Definitions

The raw 3D head data of 376 young male Chinese soldiers (aged from 19 to 23) are used [16]. All faces are aligned by translating the origin of the Cartesian coordinate system to a specified point. The y and z axis values of the new origin are the average values of the y and z axis values of sellion, both zygions, both cheilions, and menton, and the x axis value of the new origin equals the x axis value of sellion. The landmarks, defined in accordance with 1988 Anthropometric Survey of the U.S. Army Personnel Project [17], were located manually by the same experienced investigator.

Three definitions of face area are then introduced. The first method defines a face as the surface spanned from the whole heads by the front π/2 wedge angle along a line going through the centroid and pointing to the top of a head. Here the centroid was computed as the point with averaged coordinates of all points. This selection criterion of the front π/2 wedge angle is based on the observation of the average angle spanned forward of all samples in this study, based on which almost the whole face coverage could be obtained.

The second method defines a face as a grid characterized by four facial landmarks, i.e. sellion, both zygions and menton. The top of the face area lies 50mm above the sellion. This is based on the subjective judgment of the position of a full-face respirator on the forehead.

The zonal surface on the face where a certain level of compression force will be applied around is the third definition of face area for our study, since it is the actual interfacing area between equipment and face. If the surface of the contacting strip is not well consistent with the zonal surface, the compression force will be unevenly distributed and cause discomfort.

In our previous study [18], a block-division method was proposed to convert each 3D surface into a block-distance based vector. In the current case study, each face surface was divided into 30 (6X5) blocks, and the zonal surface consists of the peripheral 18 blocks.

2.2 Comparison between Different Face Area Definitions

For each face area definition, k-means clustering was applied to the block distance-based vectors referring to the inscribed surface of all samples. Wang and Yuan [19] presented a new oxygen mask sizing system where they partitioned the Chinese face samples into four sizes, namely small size, medium-narrow size, medium-wide size and large size. For comparison with their method in the future, the number of *K* for the clustering was also set as four in this case study.

The representative face surface of each cluster is obtained by calculating the average coordinates of the points of the samples belonging to the cluster. Then the block distance between a sample surface and the representative surface can be constructed as $S_1^{'}$ and $S_2^{'}$.

$S_1^{'}$ can be calculated as,

$$S_1^{'} = \frac{1}{n}\sum_{j=1}^{n} dis(p_j) \tag{1}$$

where p_j is the *j*th point, *n* represents the number of points of a face, and Euclidean distance between two corresponding points on the sample and the representative surface, $dis\ (p_j)$, was computed.

$S_2^{'}$ can be calculated as,

$$S_2' = \frac{1}{n}\sum_{j=1}^{n}\left|dis(p_j) - S_1'\right| \qquad (2)$$

S_2 describes the local shape variation between the sample and the representative surface.

Tests for normality are conducted on all S_1' and S_2' values using the One-Sample Kolmogorov-Smirnov test. Tests for the homogeneity-of-variance of the variables are conducted using the Levene test. Finally, multiple comparisons of means between the three face area definitions were conducted by using One-way ANOVA.

3 Results

3.1 Face Area Definitions

The landmarks labeled manually are illustrated in Fig. 1. Considering the difficulty in identifying landmarks on a virtual image without the ability of feeling the force feedback to palpate and locate bony landmarks as in traditional anthropometry, the landmark-label result has passed visual check from several views of the 3D head under CAD software Unigraphics.

The face areas according to the three definitions are shown in Figs. 2-4, respectively. For the zonal surface, the average value of the side length of each peripheral block is about 25mm. This is consistent with the width of the contacting strip of full-face respirator in real application.

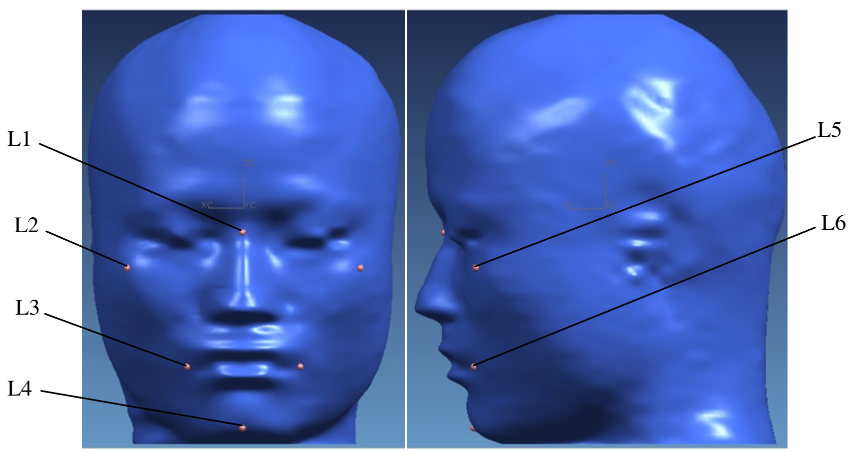

(a) front view (b) side view

Fig. 1. Interactive manual identification of landmarks (pink dots, L1: sellion; L2: right zygion; L3: right cheilion; L4: menton ; L5: left zygion; L6: left cheilion)

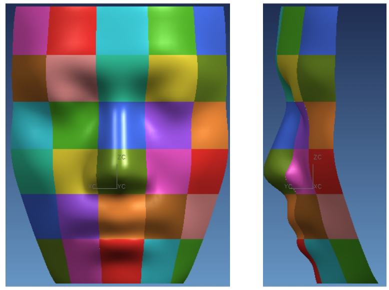

(a) front view (b) side view

Fig. 2. The first definition of face area

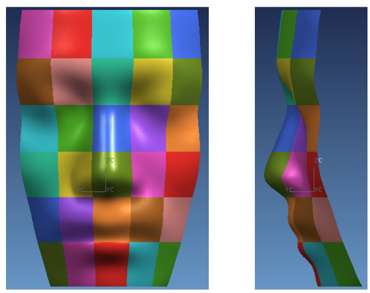

(a) front view (b) side view

Fig. 3. The second definition of face area

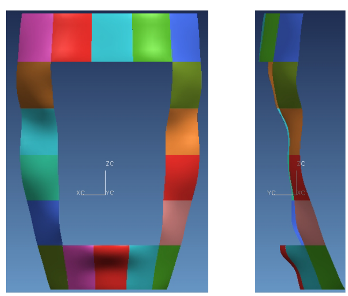

(a) front view (b) side view

Fig. 4. The third definition of face area

3.2 Comparison between Different Face Area Definitions

The average face area of each cluster was generated, as shown in Fig. 5.

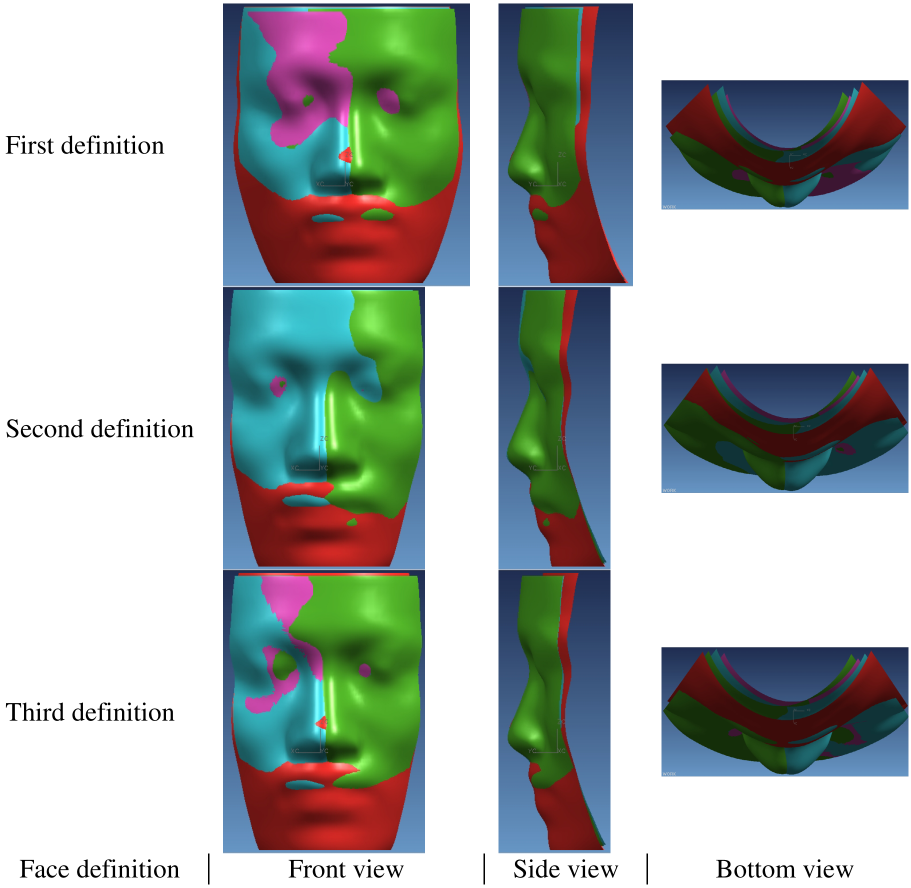

Fig. 5. Different views of the merged average faces of clusters

Tests for normality of S'_1 and S'_2 values showed p values less than 0.05, resulting in rejection of the null hypothesis. Afterwards each S'_1 and S'_2 values were transformed into their corresponding natural logarithmic values, denoted as $\ln S'_1$ and $\ln S'_2$ respectively. One-Sample Kolmogorov-Smirnov test on the $\ln S'_1$ and $\ln S'_2$ values resulted in p values greater than 0.05 (p=0.566 and 0.106 respectively). Levene test on the $\ln S'_1$ and $\ln S'_2$ values showed p values of 0.138 and 0.000, respectively. This indicated that the homogeneity-of-variance for $\ln S'_1$ was satisfied at the significance level of 0.05, while for $\ln S'_2$ the homogeneity-of-variance was not satisfied. So when multiple comparisons in One-way ANOVA was conducted, Least-significant difference (LSD) test was used for $\ln S'_1$, while Tamhane's T2 was used for $\ln S'_2$.

The descriptives of block-distance measures, i.e., $\ln S_1^{'}$ and $\ln S_2^{'}$, for different face definitions are shown in Table 1. It can be seen that for the average values of $\ln S_1^{'}$, the difference between the first two face definitions is almost ignorable. While, the average value of $\ln S_1^{'}$ for the zonal face area is greater than the first two alternatives. In contrast, the average value of $\ln S_2^{'}$ for the zonal face area is smaller than the first two alternatives. This can be explained from the definition of $S_1^{'}$ and $S_2^{'}$ which reflect the local size and shape differences, respectively. The zonal face area only covers a small portion of the whole face, i.e., the peripheral blocks of the face. For the whole face, the distance is averaged over a big surface, thus the effect of $S_1^{'}$ is weakened. Since the shape variation of the whole face is greater that that of the peripheral portion of the face, $S_2^{'}$ values of the whole face are greater. What is more, compared with the center face area consisting nose, mouth, and eyes, the zonal face area usually demonstrates more regular geometry. Therefore, the shape variation of the zonal face area is smaller, and the effect of $S_2^{'}$ is weakened.

Table 1. Descriptives of block-distance measures (*N*=376)

	Face definition	M	SD
$\ln S_1^{'}$	1	1.21	0.317
	2	1.21	0.324
	3	1.25	0.346
$\ln S_2^{'}$	1	0.09	0.383
	2	0.10	0.381
	3	0.07	0.455

As shown in Table 2, One-way ANOVA results demonstrated *p* values greater than 0.05. Such results lead to no rejection of the null hypothesis at the significance level of 0.05. However, the *p* values for $\ln S_1^{'}$ between the first and third definition (0.129), and between the second and third definition (0.070), both show marginally significant difference.

Cluster membership variation with different face areas was investigated and summarized in Table 3. Compared with the second definition, the numbers of samples whose cluster membership has changed with the first and the third definition are 83 and 30, respectively. Whereas, the number of samples with changed membership between the first and third definition is 79. It can be seen that the the membership variation between the second and third definition is much smaller than that between the first and second definition. These membership differences may indicates that the face area definition should be considered according to design requirements when developing a sizing system for face-interfaced products.

Table 2. Multiple comparisons in One-way ANOVA

Dependent Variable	Group I	Group J	Mean Difference (I-J)	Std. Error	Sig.
$\ln S_1^{'}$	1	2	0.01	0.024	0.767
	1	3	-0.04	0.024	0.129
	2	3	-0.04	0.024	0.070
$\ln S_2^{'}$	1	2	-0.02	0.028	0.894
	1	3	0.02	0.031	0.935
	2	3	0.03	0.031	0.610

Note: Group 1, 2, and 3 are the first, second and third face definitions, respectively.

Table 3. Cluster membership change (*N*=376)

Cluster ID	Sample size		
	Second definition	First definition	Third definition
1	40	37	35
2	114	160	137
3	48	48	49
4	174	131	155
number of change	-	83	30

4 Conclusions

This study investigates the influence of face area definition on 3D face shape clustering. Though no significant difference is found for the block-distance measures between these three face definitions, the cluster membership shows remarkable difference between the first definition and the latter two alternatives. This underlines the potential value of the selection of face area for assessing the face shape variation among the population and designing better fitted face-related products.

Acknowledgements

The study is supported by the National Natural Science Foundation of China (No.70571045).

References

1. Zhou, M.Q., Liu, X.N., Geng, G.H.: 3D face recognition based on geometrical measurement. In: Li, S.Z., Lai, J.-H., Tan, T., Feng, G.-C., Wang, Y. (eds.) SINOBIOMETRICS 2004. LNCS, vol. 3338, pp. 244–249. Springer, Heidelberg (2004)

2. McCloskey, E.V., Spector, T.D., Eyres, K.S., Fern, E.D., O'Rourke, N., Vasikaran, S., Kanis, J.A.: The assessment of vertebral deformity: A method for use in population studies and clinical trials. Osteoporosis International 3(3), 138–147 (1993)
3. Kaehler, K.: A Head Model with Anatomical Structure for Facial Modeling and Animation. Max-Planck-Institut für Informatik in Saarbrücken, Germany (2003)
4. Godil, A.: Advanced human body and head shape representation and analysis. In: Duffy, V.G. (ed.) HCII 2007 and DHM 2007. LNCS, vol. 4561, pp. 92–100. Springer, Heidelberg (2007)
5. Hennessy, R.J., McLearie, S., Kinsella, A., Waddington, J.L.: Facial surface analysis by 3D laser scanning and geometric morphometrics in relation to sexual dimorphism in cerebral-craniofacial morphogenesis and cognitive function. Journal of Anatomy 207(3), 283–295 (2005)
6. Hennessy, R.J., McLearie, S., Kinsella, A., Waddington, J.L.: Facial Shape and Asymmetry by Three-Dimensional Laser Surface Scanning Covary With Cognition in a Sexually Dimorphic Manner. The Journal of Neuropsychiatry and Clinical Neurosciences 18, 73–80 (2006)
7. Whitestone, J.J., Robinette, K.M.: Fitting to maximize performance of HMD systems. In: Melzer, J.E., Moffitt, K.W. (eds.) Head-Mounted Displays: Designing for the User, pp. 175–206. McGraw-Hill, New York (1997)
8. Meunier, P., Tack, D., Ricci, A., Bossi, L., Angel, H.: Helmet accommodation analysis using 3D laser scanning. Applied Ergonomics 31, 361–369 (2000)
9. Hsiao, H.W., Bradtmiller, B., Whitestone, J.: Sizing and fit of fall-protection harnesses. Ergonomics 46(12), 1233–1258 (2003)
10. Witana, C.P., Xiong, S.P., Zhao, J.H., Goonetilleke, R.S.: Foot measurements from three-dimensional scans: A comparison and evaluation of different methods. International Journal of Industrial Ergonomics 36, 789–807 (2006)
11. Au, E.Y.L., Goonetilleke, R.S.: A qualitative study on the comfort and fit of ladies' dress shoes. Applied Ergonomics 38(6), 687–696 (2007)
12. Mochimaru, M., Kouchi, M.: Proper sizing of spectacle frames based on 3-D digital faces. In: Proceedings: 15th Triennial Congress of the International Ergonomics Association (CD ROM), Seoul, Korea, August 24-29 (2003)
13. National Institute for Occupational Safety Health NIOSH, DHEW/NIOSH TR-004-73. In: McConville, J.T., Churchill, E., Laubach, L.L. (eds.) Cincinnati, OH: National Institute for Occupational Safety and Health. pp. 1–44 (1972)
14. Zhuang, Z.: Anthropometric research to support RFTPs. In: The CDC workshop on respiratory protection for airborne infectious agents, Atlanta, GA (November 2004)
15. Federal Register/Notice: Proposed Data Collections Submitted for Public Comment and Recommendations 67(16) (2002)
16. Chen, X., Shi, M.W., Zhou, H., Wang, X.T., Zhou, G.T.: The "standard head" for sizing military helmets based on computerized tomography and the headform sizing algorithm (in Chinese). Acta Armamentarii. 23(4), 476–480 (2002)
17. Cherverud, J., Gordon, C.C., Walker, R.A., Jacquish, C., Kohn, L.: Northwestern University of EVANSTON IL, 1988 Anthropometric Survey of U.S. Army Personnel: Correlation Coefficients and Regression Equations, Part 1 Statistical Techniques, Landmark and Measurement definition (TANICK/TR-90/032), pp. 48–51. U.S. Army Natick Research, Development and Engineering Center Evanston, Natick, MA (1990)
18. Niu, J.W., Li, Z.Z., Salvendy, G.: Multi-resolution shape description and clustering of three-dimensional head data. Ergonomics (in press)
19. Wang, X.W., Yuan, X.G.: Study on type and sizing tariff of aircrew oxygen masks. Journal of Beijing University of Aeronautics and Astronautics 27(3), 309–312 (2001)